

Electric dipole moment of the electron in the model with extra Higgs bosons

Noriyuki Oshimo

Department of Physics, Ochanomizu University, Tokyo, 112-8610, Japan

(Dated: May 7, 2019)

Abstract

The Higgs sector which is extended from the standard model could generally become an origin of CP violation. In the model with two doublet and one triplet Higgs fields on SU(2) symmetry, we study the electric dipole moment (EDM) of the electron whose non-vanishing value has not yet been established experimentally. The Higgs potential is assumed to be consistent with supersymmetric theory, though supersymmetric particles are not taken into consideration explicitly. While the parameter values of the model are severely constrained by the properties of the observed Higgs boson, certain ranges lead to a magnitude for the electron EDM around the experimental upper bound. Signatures of the extra Higgs bosons in collision experiments are discussed briefly.

I. INTRODUCTION

These years we have been convinced that the standard model (SM) can describe also the Higgs sector. After discovery of the Higgs boson [1], its properties have been studied extensively by experiments [2]. The production and decays proceed as the SM predicts. Quantitatively, the cross section via gluon fusion and the widths for the decays into $\bar{b}b$, WW^* , ZZ^* , and $\gamma\gamma$ are observed to be consistent with the SM. The mass measures approximately 125 GeV.

The Higgs sector, however, may not be exactly the same as the SM. Its certain extension could also yield the obtained experimental results. It would be necessary to examine the Higgs sector in great detail. If the Higgs sector is extended from the SM, some direct or indirect phenomenological appearances are expected. In particular, the interactions of Higgs bosons with quarks and leptons could violate CP invariance, which does not occur in the SM. The CP-violating phenomena may become a clue to the extended Higgs sector. Although detection of extra Higgs bosons would become unequivocal evidence, such an achievement may not be easy as the finding of the SM Higgs boson was not.

In this paper, we study the electric dipole moments (EDMs) of the electron and the neutron in the Higgs model which consists of one triplet and two doublet fields on SU(2) symmetry. Experimentally, non-vanishing value of the EDM has not been observed for the electron d^e [3] or the neutron d^n [4], and their magnitudes are bounded from above as

$$|d^e| < 8.7 \times 10^{-29} ecm, \tag{1}$$

$$|d^n| < 3.0 \times 10^{-26} ecm. \tag{2}$$

The SM predicts much smaller magnitudes. On the other hand, if CP symmetry is not conserved in the Higgs boson interactions, the EDMs of the electron and the quarks are generated at two-loop level [5]. The experimental results for the observed Higgs boson impose severe constraints on extended Higgs models. However, it will be shown that the magnitude of the electron EDM could be as large as the present experimental upper bound in sizable parameter regions of our model. The neutron EDM can not have such a large magnitude as to be comparable to the experiment. We also discuss the production and decays of the extra Higgs bosons briefly.

For Higgs bosons and their interactions with quarks and leptons, we assume the struc-

ture which are suggested at the electroweak energy scale by the supersymmetric SU(5) grand unification theory. However, our discussions are solely performed without taking into consideration supersymmetric R -odd particles, so that the obtained results can also be applied to non-supersymmetric models. Note that the Higgs sector of the minimal supersymmetric extension of the SM, although two doublet fields are contained, respects CP symmetry. Its violation occurs only through radiative corrections [6]. On the other hand, CP invariance is not conserved at tree level if the additional triplet field is introduced. All the complex coefficients of the Lagrangian cannot be made real by redefining particle fields, unless some accidental cancellation is assumed. In fact, CP-violating polarization asymmetry could be induced in the two-photon decay of the Higgs bosons in our model [7]. If supersymmetry is supposed, some non-minimal model would be implied by observation of CP violation due to the Higgs sector.

In sect. II our model is briefly described. In sect. III we obtain the EDMs of the electron and the quarks which are generated by the interactions of the Higgs bosons with the t quark and the electron or the quark. In sect. IV we perform numerical analyses for the electron EDM. Conclusion is given in sect. V. In Appendices some equations and formulae are collected.

II. MODEL

We study the electroweak model which has an extended Higgs sector with two doublet and one triplet fields for SU(2). It is assumed that the Higgs potential and the Higgs interactions with quarks and leptons are consistent with supersymmetric theory. The supersymmetric R -odd particles, however, are not taken into consideration explicitly. Either their contributions to our discussions can be neglected, or there exists no such particle.

The model contains the Higgs fields H_1 , H_2 , and Φ , which transform as $(\mathbf{2}, -1/2)$, $(\mathbf{2}, 1/2)$, and $(\mathbf{3}, 0)$ for SU(2) \times U(1) gauge symmetry,

$$H_1 = \begin{pmatrix} h_1^0 \\ h_1^- \end{pmatrix}, \quad H_2 = \begin{pmatrix} h_2^+ \\ h_2^0 \end{pmatrix}, \quad (3)$$

$$\Phi = \frac{1}{\sqrt{2}} \begin{pmatrix} \phi^0 & \sqrt{2}\phi^+ \\ \sqrt{2}\phi^- & -\phi^0 \end{pmatrix}. \quad (4)$$

We express the neutral components as

$$h_1^0 = \frac{1}{\sqrt{2}}(h_R^1 + ih_I^1), \quad h_2^0 = \frac{1}{\sqrt{2}}(h_R^2 + ih_I^2), \quad (5)$$

$$\phi^0 = \frac{1}{\sqrt{2}}(\phi_R + i\phi_I), \quad (6)$$

where the fields with index R or I are real scalar bosons. For convenience, \tilde{H}_1 is defined by

$$\tilde{H}_1 = \begin{pmatrix} h_1^{-*} \\ -h_1^{0*} \end{pmatrix},$$

whose transformation property is of $(\mathbf{2}, 1/2)$. Assuming that electromagnetic symmetry is not broken, we write the vacuum expectation values (VEVs) of the neutral Higgs fields as

$$\langle h_1^0 \rangle = v_1 e^{i\theta_1}, \quad \langle h_2^0 \rangle = v_2 e^{i\theta_2}, \quad \langle \phi^0 \rangle = v_0 e^{i\theta_0}, \quad (7)$$

where v_1 , v_2 , and v_0 denote absolute values. The ratio of v_2 to v_1 is expressed by $\tan \beta = v_2/v_1$. These absolute values are constrained by the masses of the Z and W bosons, whose relations are given by

$$M_Z = \frac{1}{\sqrt{2}} \sqrt{(g^2 + g'^2)(v_1^2 + v_2^2)}, \quad (8)$$

$$M_W = \frac{1}{\sqrt{2}} g \sqrt{v_1^2 + v_2^2 + 4v_0^2}. \quad (9)$$

The ρ parameter becomes

$$\rho = \frac{g^2 + g'^2}{g^2} \frac{M_W^2}{M_Z^2} = \frac{v_1^2 + v_2^2 + 4v_0^2}{v_1^2 + v_2^2}, \quad (10)$$

which indicates the relation between the masses of the Z and W bosons. With $\tan \beta$ being a free parameter, the values of v_1 and v_2 are determined. We take v_0 for 3 GeV, which is almost a maximum value allowed experimentally.

The Higgs potential is expressed as

$$V = V_0 + V_1, \quad (11)$$

corresponding to the terms at tree level V_0 and at one-loop level V_1 in supersymmetric theory. The first term is given by

$$V_0 = M_1^2 |\tilde{H}_1|^2 + M_2^2 |H_2|^2 + M_3^2 \text{Tr}[\Phi^\dagger \Phi] \\ + \left(m_1^2 \tilde{H}_1^\dagger H_2 + \frac{1}{2} m_2^2 \text{Tr}[\Phi^2] + \text{H.c.} \right)$$

$$\begin{aligned}
& + \left\{ \lambda \mu_H^* (\tilde{H}_1^\dagger \Phi \tilde{H}_1 + H_2^\dagger \Phi H_2) + \lambda \mu_\phi^* \tilde{H}_1^\dagger \Phi^\dagger H_2 + m_3 \tilde{H}_1^\dagger \Phi H_2 + \text{H.c.} \right\} \\
& + \frac{1}{8} (g^2 + g'^2) (|\tilde{H}_1|^4 + |H_2|^4) \\
& + \left\{ \frac{1}{4} (g^2 - g'^2) + |\lambda|^2 \right\} |\tilde{H}_1|^2 |H_2|^2 - \frac{1}{2} (g^2 + |\lambda|^2) |\tilde{H}_1^\dagger H_2|^2 \\
& + \frac{1}{2} g^2 \text{Tr}[\Phi^\dagger (\Phi \Phi^\dagger - \Phi^\dagger \Phi) \Phi] \\
& + \left(-\frac{1}{2} g^2 + |\lambda|^2 \right) \tilde{H}_1^\dagger \Phi \Phi^\dagger \tilde{H}_1 + \frac{1}{2} g^2 \tilde{H}_1^\dagger \Phi^\dagger \Phi \tilde{H}_1 \\
& + \left(-\frac{1}{2} g^2 + |\lambda|^2 \right) H_2^\dagger \Phi^\dagger \Phi H_2 + \frac{1}{2} g^2 H_2^\dagger \Phi \Phi^\dagger H_2, \tag{12}
\end{aligned}$$

$$M_1^2 = |\mu_H|^2 + \text{Re}(M_{H1}^2), \quad M_2^2 = |\mu_H|^2 + \text{Re}(M_{H2}^2), \quad M_3^2 = |\mu_\phi|^2 + \text{Re}(M_\Phi^2),$$

where g and g' stand for the gauge coupling constants for SU(2) and U(1), respectively. The parameters M_{H1}^2 , M_{H2}^2 , and M_Φ^2 are of mass-squared dimension. The dimensionless parameter λ and the mass parameters μ_H , μ_ϕ , and m_i ($i=1-3$) all have complex values generally. This tree level potential, however, does not describe well the neutral Higgs bosons. It is necessary to incorporate additional terms, which may come from radiative corrections in supersymmetric theory [8]. In the one-loop potential, the terms which are relevant to the neutral Higgs bosons are given, in simplified form, by

$$\begin{aligned}
V_1 \supset & -\frac{3}{16\pi^2} m_t^4 \left(\log \frac{m_t^2}{\Lambda^2} + \frac{1}{2} \right) \\
& + \frac{3}{32\pi^2} M_{t1}^4 \left(\log \frac{M_{t1}^2}{\Lambda^2} + \frac{1}{2} \right) + \frac{3}{32\pi^2} M_{t2}^4 \left(\log \frac{M_{t2}^2}{\Lambda^2} + \frac{1}{2} \right). \tag{13}
\end{aligned}$$

Here, m_t denotes the t -quark mass, which is expressed as

$$m_t^2 = |\eta_t|^2 v_2^2, \tag{14}$$

with η_t being a coupling constant; M_{ti}^2 ($i=1,2$) are given by

$$M_{t1}^2 = |\eta_t|^2 v_2^2 + \text{Re}(M_Q^2), \quad M_{t2}^2 = |\eta_t|^2 v_2^2 + \text{Re}(M_{Uc}^2), \tag{15}$$

where M_Q^2 and M_{Uc}^2 stand for mass-squared parameters; and Λ is an appropriate energy scale. This energy scale is taken as

$$-2m_t^2 \left(\log \frac{m_t^2}{\Lambda^2} + 1 \right) + M_{t1}^2 \left(\log \frac{M_{t1}^2}{\Lambda^2} + 1 \right) + M_{t2}^2 \left(\log \frac{M_{t2}^2}{\Lambda^2} + 1 \right) = 0, \tag{16}$$

which makes the extremum conditions for the VEVs manageable.

In general, the Higgs potential has five complex coefficients $\lambda\mu_H^*$, $\lambda\mu_\phi^*$, and m_i ($i=1-3$). Although two coefficients can be made real by redefining phases of the fields, the others remain complex, leading to CP violation. Without loss of generality, we can define $m_1^2 = |m_1^2|$, $m_2^2 = -|m_2^2|$, $\lambda\mu_H^* = |\lambda\mu_H^*|e^{i\alpha_1}$, $\lambda\mu_\phi^* = |\lambda\mu_\phi^*|e^{i\alpha_2}$, and $m_3 = |m_3|e^{i\alpha_3}$, taking m_1^2 and m_2^2 for real. Owing to the complex coefficients, the VEVs of the Higgs fields in Eq. (7) become complex. The extremum conditions for the VEVs are given in Appendix A. In our scheme the complex phases θ_1 and θ_2 appear as a linear combination $\theta_1 + \theta_2$ ($\equiv \theta$) in the potential, so that only the phase θ is determined at the vacuum.

The mass eigenstates for Higgs bosons are determined by the potential V in Eq. (11). The mass-squared matrices for the neutral Higgs bosons and the charged Higgs bosons are expressed respectively by a 6×6 real symmetric matrix \mathcal{M}^0 in Appendix B and by a 4×4 Hermitian matrix \mathcal{M}^\pm in Appendix C. These matrices are diagonalized by an orthogonal matrix O and by a unitary matrix U ,

$$O^T \mathcal{M}^0 O = \text{diag} \left(\tilde{M}_{H1}^{02}, \tilde{M}_{H2}^{02}, \tilde{M}_{H3}^{02}, \tilde{M}_{H4}^{02}, \tilde{M}_{H5}^{02}, \tilde{M}_{H6}^{02} \right), \quad (17)$$

$$U^\dagger \mathcal{M}^\pm U = \text{diag} \left(\tilde{M}_{H1}^{\pm 2}, \tilde{M}_{H2}^{\pm 2}, \tilde{M}_{H3}^{\pm 2}, \tilde{M}_{H4}^{\pm 2} \right), \quad (18)$$

where the eigenvalues are in ascending order. The neutral Higgs bosons \tilde{H}_i^0 and the charged Higgs bosons \tilde{H}_i^- in mass eigenstates are then expressed as

$$\tilde{H}_i^0 = O_{1i} h_R^1 + O_{2i} h_R^2 + O_{3i} \phi_R + O_{4i} h_I^1 + O_{5i} h_I^2 + O_{6i} \phi_I, \quad (19)$$

$$\tilde{H}_i^- = U_{1i}^* h_1^- + U_{2i}^* h_2^{+*} + U_{3i}^* \phi^- + U_{4i}^* \phi^{+*}. \quad (20)$$

The Goldstone bosons for spontaneous breaking of SU(2) symmetry are represented by \tilde{H}_1^0 and \tilde{H}_1^- , and the values of \tilde{M}_{H1}^{02} and $\tilde{M}_{H1}^{\pm 2}$ vanish. In the neutral mass eigenstates, the CP-even and CP-odd fields are mixed.

Neglecting the generation mixing, the interaction Lagrangian for the neutral Higgs bosons with the quarks and the charged lepton of the first generation is given by

$$\begin{aligned} \mathcal{L} = & -\frac{m_u}{\sqrt{2}v_2} \bar{\psi}_u \left(F_u^i \frac{1-\gamma_5}{2} + F_u^{i*} \frac{1+\gamma_5}{2} \right) \psi_u \tilde{H}_i^0 \\ & -\frac{m_d}{\sqrt{2}v_1} \bar{\psi}_d \left(F_d^i \frac{1-\gamma_5}{2} + F_d^{i*} \frac{1+\gamma_5}{2} \right) \psi_d \tilde{H}_i^0 \\ & -\frac{m_e}{\sqrt{2}v_1} \bar{\psi}_e \left(F_e^i \frac{1-\gamma_5}{2} + F_e^{i*} \frac{1+\gamma_5}{2} \right) \psi_e \tilde{H}_i^0, \quad (21) \\ F_u^i = & e^{-i\theta_2} (O_{2i} + iO_{5i}), \quad F_d^i = F_e^i = e^{-i\theta_1} (O_{1i} + iO_{4i}), \end{aligned}$$

where m_u , m_d , and m_e denote the masses of the u quark, d quark, and electron, respectively. Even if generation mixing is absent, CP invariance is not respected. The interactions for the other generations of quarks and charged leptons are obtained by exchanging the masses, while the coefficients F_u^i and F_d^i (F_e^i) remain the same. The interaction Lagrangian for the Higgs bosons and the W or Z boson is given by

$$\begin{aligned} \mathcal{L} &= gM_W \sqrt{\frac{v_1^2 + v_2^2}{v_1^2 + v_2^2 + 4v_0^2}} G_W^i W^{+\mu} W_\mu^- \tilde{H}_i^0 + \frac{1}{2} \sqrt{g^2 + g'^2} M_Z G_Z^i Z^\mu Z_\mu \tilde{H}_i^0, \quad (22) \\ G_W^i &= \cos \beta (O_{1i} \cos \theta_1 + O_{4i} \sin \theta_1) + \sin \beta (O_{2i} \cos \theta_2 + O_{5i} \sin \theta_2) \\ &\quad + \frac{4v_0}{\sqrt{v_1^2 + v_2^2}} (O_{3i} \cos \theta_0 + O_{6i} \sin \theta_0), \\ G_Z^i &= \cos \beta (O_{1i} \cos \theta_1 + O_{4i} \sin \theta_1) + \sin \beta (O_{2i} \cos \theta_2 + O_{5i} \sin \theta_2). \end{aligned}$$

The Z boson does not couple to the SU(2)-triplet Higgs fields ϕ_R and ϕ_I .

III. ELECTRIC DIPOLE MOMENT

The interactions of the neutral Higgs bosons \tilde{H}_i^0 ($i=2-6$) and the quarks or charged leptons could induce various CP-violating phenomena. In particular, sizable effects may be yielded by the processes which quarks of the third generation participate in, since the coupling constants are generally proportional to the masses and thus non-negligible. The EDM is such a quantity. The EDM of the electron could be generated at two-loop level by the diagrams mediated by the t quark as shown in Fig. 1. Similar diagrams could also lead to non-negligible values for the EDMs of the u quark and d quark, which may be observed as the EDM of the neutron.

The EDM d^f of the electron, u quark, or d quark with electric charge eQ_f and mass m_f is given by

$$\begin{aligned} \frac{d^f}{e} &= \left(\frac{gg'}{12\pi^2} \right)^2 \frac{1}{\sin 2\beta} \frac{Q_f m_f}{M_Z^2} \sum_{i=2}^6 r_t^i \left[\text{Re}(F_f^i) \text{Im}(F_u^i) I(r_t^i) + \text{Im}(F_f^i) \text{Re}(F_u^i) J(r_t^i, r_f^i) \right], \quad (23) \\ r_t^i &= \frac{m_t^2}{\tilde{M}_{H_i}^{02}}, \quad r_f^i = \frac{m_f^2}{\tilde{M}_{H_i}^{02}}, \end{aligned}$$

where F_f^i denotes an appropriate coupling constant in Eq. (21), with e being the elementary electric charge. The functions are defined by

$$I(r_t) = \frac{1}{2} \int_0^1 ds \frac{1-s}{s(1-s)-r_t} \log \frac{s(1-s)}{r_t}, \quad (24)$$

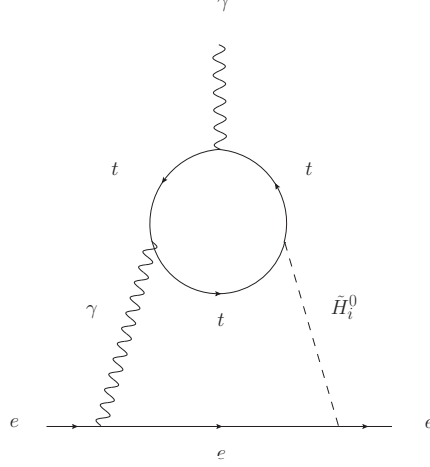


FIG. 1: The two-loop diagram for the EDM of the electron. Another diagram in which the photon and the Higgs boson lines are interchanged also gives a contribution.

$$\begin{aligned}
J(r_t, r_f) &= J_1 + J_2, \tag{25} \\
J_1 &= -\frac{1}{4} \int_0^1 ds \frac{1-s}{s(1-s) - r_t} \left\{ s^2 + \left[r_t - 2 + 3s - 4s^2 - \frac{(s-r_t)r_t}{s(1-s) - r_t} \right] \log \frac{s(1-s)}{r_t} \right\}, \\
J_2 &= \frac{1}{2} \iint_D ds dt \frac{1-s}{\tau^3} r_t \times \\
&\quad \left(\sqrt{\frac{\tau}{r_f r_t}} \left\{ 2 + [4r_t - 2 + s(1-s)]t \right\} \arctan \sqrt{\frac{r_f}{\tau r_t}} (1-t) \right. \\
&\quad + \frac{1}{1 + \sqrt{\sigma}} \left\{ [4(1-r_t) - s(1-s)]t - 4 - \frac{s(1-s)t}{\sqrt{\sigma}} \right\} \log \frac{1 - (1-r_t)t}{r_t} \\
&\quad + \frac{1}{\sqrt{\sigma}} \left\{ \frac{\tau}{r_f} - 4 + [4(1-r_f) - s(1-s)]t \right\} \times \\
&\quad \quad \left. \left\{ \log \left[1 - \frac{2r_f(1-t)}{\tau(1 + \sqrt{\sigma})} \right] - \log \left[1 + \frac{2r_f(1-t)}{\tau(1 + \sqrt{\sigma})} \frac{1 - (1-r_t)t}{r_t} \right] \right\} \right), \\
\tau &= 1 - (s^2 - s + 1)t, \quad \sigma = 1 - 4r_e \frac{1 - (1-r_t)t}{1 - (s^2 - s + 1)t}.
\end{aligned}$$

In these functions the terms which are trivially proportional to r_f have been discarded. The integral domain D is approximately given by

$$D : 0 \leq s \leq 1, \quad 0 \leq t \leq 1,$$

where small regions proportional to r_f are also neglected.

We can evaluate roughly the magnitude of the EDM in Eq. (23). The electron mass

measures $m_e = 5.1 \times 10^{-4}$ GeV, so that the EDM of the electron is proportional to a factor

$$\left(\frac{gg'}{12\pi^2}\right)^2 \frac{1}{\sin 2\beta} \frac{m_e}{M_Z^2} \simeq 4.8 \times 10^{-27} \text{cm}$$

for $\tan \beta = 10$. This factor is much larger than the experimental bound. Therefore, the CP violating phases α_i ($i=1-3$) should have such values as to make $\text{Re}(F_e^i)\text{Im}(F_u^i)$ and $\text{Im}(F_e^i)\text{Re}(F_u^i)$ less than of order of 10^{-2} . Depending on the phases, the predicted magnitude of the EDM at two-loop level could have any value below the experimental bound.

The EDM of the neutron is described by the EDMs of the quarks. The masses of the u quark and d quark measure roughly $m_u = 2.2 \times 10^{-3}$ GeV and $m_d = 4.7 \times 10^{-3}$ GeV [9]. Since the first approximation of the neutron EDM is given by $d^n = (4d^d - d^u)/3$, its magnitude is estimated at most to be the experimental bound. If the CP violating phases are constrained to keep the EDM of the electron consistent with the experiment, the neutron EDM would be much smaller than the bound. We therefore do not make numerical analyses for the neutron EDM any more.

IV. NUMERICAL ANALYSES

The prediction of the EDMs depend on model parameters, which are constrained by various experimental results. First, by the extremum conditions of the potential in Appendix A, we can express the mass-squared parameters $\text{Re}(M_{H1}^2)$, $\text{Re}(M_{H2}^2)$, $\text{Re}(M_{\Phi}^2)$, $|m_1^2|$, and $|m_2^2|$ in terms of the VEVs of the Higgs bosons v_1 , v_2 , v_0 , θ ($= \theta_1 + \theta_2$), and θ_0 in Eq. (7) and the parameters $|\lambda|$, $|\mu_H|$, $|\mu_\phi|$, $|m_3|$, and α_i ($i=1-3$). The absolute values v_1 , v_2 , and v_0 should give the masses of the W and Z bosons in Eqs. (8) and (9). The parameters $\text{Re}(M_Q^2)$ and $\text{Re}(M_{Uc}^2)$ in Eq. (15) are left free.

A severe constraint comes from the SM Higgs boson which is observed experimentally. We take the lightest Higgs boson \tilde{H}_2^0 for this particle. Assuming that the Higgs boson is produced dominantly through the gluon fusion mediated by the t quark, the cross section $\sigma(\tilde{H}_2^0)$ is proportional roughly to the square of the coupling constant for t and \bar{t} . The decay widths for $\bar{b}b$, WW^* , and ZZ^* are also proportional to the squares of their coupling constants. Since the Higgs boson decays dominantly into b and \bar{b} , the branching ratios $\text{Br}(WW^*)$ and $\text{Br}(ZZ^*)$ may be given by the ratios of their widths to the width for $\bar{b}b$. Therefore, concerning production and decay, the ratios of this model to the SM could be

estimated roughly by the ratios of the squared coupling constants .

The experiments for the Higgs boson have found that its production cross section and decay branching ratios are consistent with the prediction by the SM. Allowing for uncertainty of our scheme and experimental results, we impose the following constraints on the parameters,

$$\tilde{M}_{H_2}^0 = 120 - 130 \text{ [GeV]}, \quad (26)$$

$$\frac{\sigma(\tilde{H}_2^0)}{\sigma_{SM}(\tilde{H}_2^0)} \simeq \frac{v_1^2 + v_2^2 + 4v_0^2}{v_2^2} |F_u^2|^2 = 0.8 - 1.2, \quad (27)$$

$$\frac{\sigma(\tilde{H}_2^0) \cdot \text{Br}(WW^*)}{\sigma_{SM}(\tilde{H}_2^0) \cdot \text{Br}_{SM}(WW^*)} \simeq \cot^2 \beta \frac{v_1^2 + v_2^2}{v_1^2 + v_2^2 + 4v_0^2} \frac{|F_u^2|^2}{|F_d^2|^2} (G_W^2)^2 = 0.8 - 1.2, \quad (28)$$

$$\frac{\sigma(\tilde{H}_2^0) \cdot \text{Br}(ZZ^*)}{\sigma_{SM}(\tilde{H}_2^0) \cdot \text{Br}_{SM}(ZZ^*)} \simeq \cot^2 \beta \frac{|F_u^2|^2}{|F_d^2|^2} (G_Z^2)^2 = 0.8 - 1.2. \quad (29)$$

Here, σ_{SM} and Br_{SM} denote the cross section and the branching ratio under the SM interactions, with $\tilde{M}_{H_2}^0$ being taken for the Higgs boson mass. The decay width for $\bar{b}b$ receives non-negligible contributions from QCD corrections [10]. However, the above estimate uses the ratio for the two models, which is not affected much by the corrections. The measurements for the branching ratio of $\tilde{H}_2^0 \rightarrow \gamma\gamma$ give values around the SM prediction of 2×10^{-3} . The interactions relevant to this decay induce also the production of the Higgs boson and its decay into WW^* . Under the parameter values constrained from Eqs. (26)-(29), the branching ratio $\text{Br}(\gamma\gamma)$ becomes compatible with the experimental result.

In Fig. 2 the absolute value of the electron EDM is shown as a function of θ for $0 < \theta < \pi/2$ with $\theta_0 = \pi/12$. The experimental constraints on the Higgs boson \tilde{H}_2^0 are satisfied in sizable regions of the parameter space. We show two examples (a) $|\mu_H| = |\mu_\phi| = 300$ GeV and (b) $|\mu_H| = |\mu_\phi| = 1000$ GeV, with $|m_3| = \text{Re}(M_Q^2) = \text{Re}(M_{U^c}^2) = 1000$ GeV and $|\lambda| = 1$. The ratio of the VEVs is fixed at a typical value $\tan \beta = 10$. With the phases α_1, α_2 , and α_3 being varied from 0 to 2π , if the vacuum is consistent with the experimental constraints, excepting the upper bound on the EDM in Eq. (1), the absolute value of the EDM is depicted as a point. As the complex phases of the VEVs increase, the magnitude of the EDM becomes large. The predicted magnitude is inside the experimental bound for smaller values of θ , while outside for larger values. For $0.3 < \theta$ and $0.2 < \theta$ in Figs. 2 (a) and 2 (b), respectively, the parameter values do not satisfy the experimental results for the observed Higgs boson.

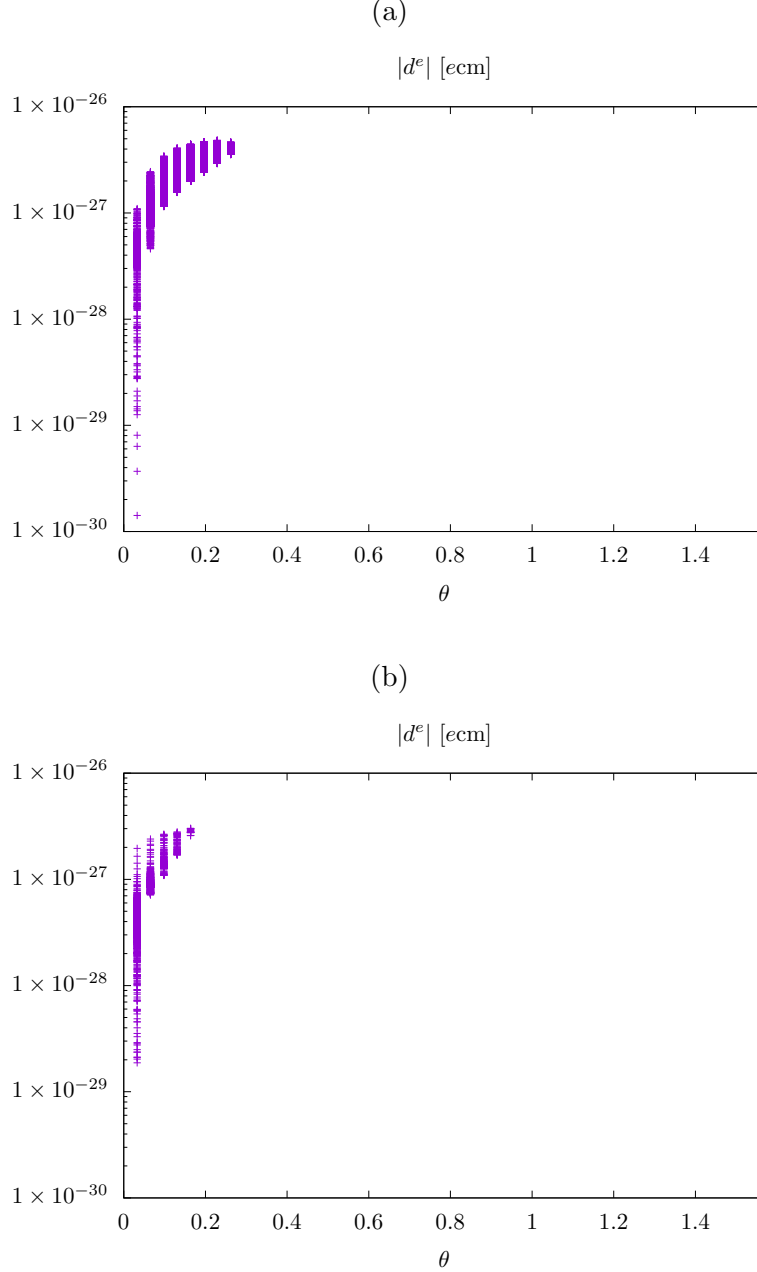


FIG. 2: The absolute value of the electron EDM as a function of the phase θ , with $\theta_0 = \pi/12$.

(a) $|\mu_H| = |\mu_\phi| = 300$ GeV, (b) $|\mu_H| = |\mu_\phi| = 1000$ GeV.

In Table I two examples are shown for specific phase values. The other parameter values of examples (a) and (b) are the same as (a) and (b) of Fig. 2, respectively. In general, the parameter values of the model is constrained severely by the experimental results for the observed Higgs boson. In spite of this constraint, within the allowed region, the EDM can have a magnitude around the present experimental upper bound.

TABLE I: The values of CP-violating phases and the electron EDM. (a) $|\mu_H| = |\mu_\phi| = 300$ GeV, (b) $|\mu_H| = |\mu_\phi| = 1000$ GeV.

	α_1	α_2	α_3	θ_0	θ	$ d^e $ [ecm]
(a)	$-\frac{3}{8}\pi$	$\frac{5}{6}\pi$	$-\frac{1}{8}\pi$	$\frac{1}{12}\pi$	$\frac{1}{96}\pi$	8.4×10^{-29}
(b)	$-\frac{1}{2}\pi$	$\frac{11}{48}\pi$	$-\frac{47}{48}\pi$	$\frac{1}{12}\pi$	$\frac{1}{96}\pi$	5.9×10^{-29}

In the present model there exist four extra neutral Higgs bosons \tilde{H}_i^0 ($i=3-6$). The cross sections are roughly proportional to the squares of the coupling coefficients with the t quark or with the b quark in Eq. (21). The ratios of these squares to those corresponding to the SM are given by

$$R_t = \frac{v_1^2 + v_2^2 + 4v_0^2}{v_2^2} |F_u^i|^2, \quad R_b = \frac{v_1^2 + v_2^2 + 4v_0^2}{v_1^2} |F_d^i|^2, \quad (30)$$

for the t and b quarks. In Table II these ratios and the branching ratios for $\tilde{H}_i^0 \rightarrow \bar{b}b, \bar{t}t, W^+W^-, ZZ$ are given, together with the mass values, for the examples (a) and (b). Compared to the SM interactions, the magnitude of the interaction with the t quark is small, while that with the b quark is large. Therefore, the cross sections of the gluon fusion $gg \rightarrow \tilde{H}_i^0$ mediated by the t quark are suppressed, while the cross sections of the gluon fusion mediated by the b quark and of the associated production $gg \rightarrow \bar{b}b\tilde{H}_i^0$ are enhanced. A naive estimate gives that the cross section would be small by a factor of order of 10^{-1} compared to the t -quark mediated gluon fusion in the SM. The decay properties are also different from the SM. The decay into $\bar{b}b$ has the largest branching ratio, while in the SM the Higgs-like boson with a mass larger than about 200 GeV decays dominantly into W^+W^- and ZZ .

Experiments have not observed a Higgs-like boson, except the observed one, for the mass range smaller than 1000 GeV [11], provided that the phenomena are described like the Higgs boson of the SM. Although some of the extra Higgs bosons have mass values within the excluded range, the production cross sections become generally small and the branching ratios are different from the SM. The experimental negative results could not apply to the extra bosons.

This model predicts also three charged Higgs bosons. Experiments have not found such a boson, and the lower bound on the mass is obtained as 80 GeV [12]. On the other hand,

TABLE II: The masses, branching ratios, and ratios for coupling strengths of the neutral Higgs bosons for examples (a) and (b). The lightest particle corresponds to the observed Higgs boson.

mass [GeV]	$\bar{b}b$	$\bar{t}t$	W^+W^-	ZZ	R_t	R_b
(a)						
123	1.0	0	0	0	9.9×10^{-1}	1.0
178	9.7×10^{-1}	0	3.4×10^{-2}	0	1.5×10^{-2}	9.4×10
222	9.9×10^{-1}	0	4.5×10^{-3}	1.8×10^{-3}	9.3×10^{-3}	1.0×10^2
607	4.4×10^{-1}	2.0×10^{-1}	2.6×10^{-1}	9.7×10^{-2}	3.1×10^{-3}	6.4
247×10	8.9×10^{-3}	2.4×10^{-2}	6.5×10^{-1}	3.2×10^{-1}	1.1×10^{-4}	6.5×10^{-2}
(b)						
121	1.0	0	0	0	1.0	1.0
193	1.0	0	5.1×10^{-8}	4.8×10^{-4}	1.1×10^{-2}	7.9×10
281	1.0	0	1.6×10^{-4}	7.0×10^{-5}	9.0×10^{-3}	1.0×10^2
478	8.2×10^{-1}	8.3×10^{-2}	6.9×10^{-2}	2.9×10^{-2}	1.9×10^{-3}	2.1×10
497×10	2.8×10^{-4}	5.3×10^{-3}	6.6×10^{-1}	3.3×10^{-1}	9.0×10^{-5}	8.1×10^{-3}

TABLE III: The masses [GeV] of the charged Higgs bosons for examples (a) and (b).

(a)	222	608	247×10
(b)	235	483	497×10

the masses of the charged Higgs bosons in our model become generally larger than 100 GeV. In Table III the mass values are listed for examples (a) and (b). There may exist a charged Higgs boson whose mass is not much above the excluded range.

V. CONCLUSION

We have studied the EDM of the electron, assuming the extension of the SM which has the Higgs fields of two doublet and one triplet representations for SU(2) transformation.

The extended Higgs sector induces naturally violation of CP invariance at tree level. As a result, charged leptons and quarks could have non-vanishing EDMs at two-loop level, which are mediated by the Higgs bosons and the t quark. On the other hand, the extended sector is severely constrained from the experimental results for the observed Higgs boson. The EDM of the electron has not been observed and its upper bound on the magnitude is obtained. We have found the region of parameter space which is consistent with the Higgs boson and gives a large magnitude for the EDM. The EDM can be expected to have a magnitude around the present experimental bound.

Possible CP violating effects in the SM are very restricted. If the Higgs sector does not conserve CP invariance, the resultant phenomena would be easily distinguished from the SM. One example is the EDM of the electron or the neutron. The two-photon decay of the Higgs boson may also show CP asymmetry for the helicities. Important clues for physics beyond the SM may be provided by examining CP violation.

Our model predicts extra neutral Higgs bosons, which could have escaped detection in experiments. The production and decay properties of these bosons are different much from the SM Higgs boson. Their production cross sections by the gluon fusion generally become smaller. The dominant decay modes are $\bar{b}b$, and not W^+W^- and ZZ , even if kinematically allowed. In order to detect the extra Higgs bosons, it would be necessary to make experimental analyses which are different from those for searching a Higgs-like boson of the SM.

Appendix A: Extremum conditions

The extremum conditions $\partial V/\partial v_1$, $\partial V/\partial v_2$, $\partial V/\partial v_0$, $\partial V/\partial \theta$, and $\partial V/\partial \theta_0$ are given by

$$M_1^2 + \frac{g^2 + g'^2}{4} v_1^2 - \left(\frac{g^2 + g'^2}{4} - \frac{|\lambda|^2}{2} \right) v_2^2 + \frac{|\lambda|^2}{2} v_0^2 - \sqrt{2} v_0 |\lambda \mu_H^*| \cos(\alpha_1 + \theta_0) = \frac{v_2}{v_1} \left\{ |m_1^2| \cos \theta - \frac{v_0}{\sqrt{2}} \left[|\lambda \mu_\phi^*| \cos(\alpha_2 - \theta_0 + \theta) + |m_3| \cos(\alpha_3 + \theta_0 + \theta) \right] \right\}, \quad (\text{A1})$$

$$M_2^2 + \frac{g^2 + g'^2}{4} v_2^2 - \left(\frac{g^2 + g'^2}{4} - \frac{|\lambda|^2}{2} \right) v_1^2 + \frac{|\lambda|^2}{2} v_0^2 - \sqrt{2} v_0 |\lambda \mu_H^*| \cos(\alpha_1 + \theta_0) = \frac{v_1}{v_2} \left\{ |m_1^2| \cos \theta - \frac{v_0}{\sqrt{2}} \left[|\lambda \mu_\phi^*| \cos(\alpha_2 - \theta_0 + \theta) + |m_3| \cos(\alpha_3 + \theta_0 + \theta) \right] \right\}, \quad (\text{A2})$$

$$M_3^2 + \frac{|\lambda|^2}{2} (v_1^2 + v_2^2) - |m_2^2| \cos 2\theta_0 - \frac{v_1^2 + v_2^2}{\sqrt{2} v_0} |\lambda \mu_H^*| \cos(\alpha_1 + \theta_0) =$$

$$-\frac{v_1 v_2}{\sqrt{2} v_0} \left\{ |\lambda m_\phi^*| \cos(\alpha_2 - \theta_0 + \theta) + |m_3| \cos(\alpha_3 + \theta_0 + \theta) \right\}, \quad (\text{A3})$$

$$|m_1^2| \sin \theta = \frac{v_0}{\sqrt{2}} \left\{ |\lambda \mu_\phi^*| \sin(\alpha_2 - \theta_0 + \theta) + |m_3| \sin(\alpha_3 + \theta_0 + \theta) \right\}, \quad (\text{A4})$$

$$\begin{aligned} |m_2^2| \sin 2\theta_0 + \frac{v_1^2 + v_2^2}{\sqrt{2} v_0} |\lambda \mu_H^*| \sin(\alpha_1 + \theta_0) = \\ -\frac{v_1 v_2}{\sqrt{2} v_0} \left\{ |\lambda \mu_\phi^*| \sin(\alpha_2 - \theta_0 + \theta) - |m_3| \sin(\alpha_3 + \theta_0 + \theta) \right\}. \end{aligned} \quad (\text{A5})$$

Since the equations $\langle \partial V_1 / \partial h_R^2 \rangle = \langle \partial V_1 / \partial h_I^2 \rangle = 0$ are derived from the assumption in Eq. (16), these extremum conditions are the same as those for the tree-level potential V_0 .

Appendix B: Mass-squared matrix for the neutral Higgs bosons

The mass-squared matrix \mathcal{M}^0 for the neutral Higgs bosons receives contributions from the tree-level potential and the one-loop potential, $\mathcal{M}^0 = \mathcal{M}^{0(0)} + \mathcal{M}^{0(1)}$. The elements M_{ij}^0 are given by

$$\begin{aligned} \mathcal{M}_{11}^{0(0)} = M_1^2 + \frac{g^2 + g'^2}{4} (1 + 2 \cos^2 \theta_1) v_1^2 - \left(\frac{g^2 + g'^2}{4} - \frac{|\lambda|^2}{2} \right) v_2^2 \\ + \frac{|\lambda|^2}{2} v_0^2 - \sqrt{2} v_0 |\lambda \mu_H^*| \cos(\alpha_1 + \theta_0), \end{aligned} \quad (\text{B1})$$

$$\begin{aligned} \mathcal{M}_{12}^{0(0)} = -\left(\frac{g^2 + g'^2}{2} - |\lambda|^2 \right) v_1 v_2 \cos \theta_1 \cos \theta_2 - |m_1^2| \\ + \frac{v_0}{\sqrt{2}} \left\{ |\lambda \mu_\phi^*| \cos(\alpha_2 - \theta_0) + |m_3| \cos(\alpha_3 + \theta_0) \right\}, \end{aligned} \quad (\text{B2})$$

$$\begin{aligned} \mathcal{M}_{13}^{0(0)} = |\lambda|^2 v_1 v_0 \cos \theta_1 \cos \theta_0 - \sqrt{2} v_1 |\lambda \mu_H^*| \cos \alpha_1 \cos \theta_1 \\ + \frac{v_2}{\sqrt{2}} \left\{ |\lambda \mu_\phi^*| \cos(\alpha_2 + \theta_2) + |m_3| \cos(\alpha_3 + \theta_2) \right\}, \end{aligned} \quad (\text{B3})$$

$$\mathcal{M}_{14}^{0(0)} = \frac{g^2 + g'^2}{4} v_1^2 \sin 2\theta_1, \quad (\text{B4})$$

$$\begin{aligned} \mathcal{M}_{15}^{0(0)} = -\left(\frac{g^2 + g'^2}{2} - |\lambda|^2 \right) v_1 v_2 \cos \theta_1 \sin \theta_2 \\ - \frac{v_0}{\sqrt{2}} \left\{ |\lambda \mu_\phi^*| \sin(\alpha_2 - \theta_0) + |m_3| \sin(\alpha_3 + \theta_0) \right\}, \end{aligned} \quad (\text{B5})$$

$$\begin{aligned} \mathcal{M}_{16}^{0(0)} = |\lambda|^2 v_1 v_0 \cos \theta_1 \sin \theta_0 + \sqrt{2} v_1 |\lambda \mu_H^*| \sin \alpha_1 \cos \theta_1 \\ + \frac{v_2}{\sqrt{2}} \left\{ |\lambda \mu_\phi^*| \sin(\alpha_2 + \theta_2) - |m_3| \sin(\alpha_3 + \theta_2) \right\}, \end{aligned} \quad (\text{B6})$$

$$\begin{aligned} \mathcal{M}_{22}^{0(0)} = M_2^2 + \frac{g^2 + g'^2}{4} v_2^2 (1 + 2 \cos^2 \theta_2) - \left(\frac{g^2 + g'^2}{4} - \frac{|\lambda|^2}{2} \right) v_1^2 \\ + \frac{|\lambda|^2}{2} v_0^2 - \sqrt{2} v_0 |\lambda \mu_H^*| \cos(\alpha_1 + \theta_0), \end{aligned} \quad (\text{B7})$$

$$\mathcal{M}_{23}^{0(0)} = |\lambda|^2 v_2 v_0 \cos \theta_2 \cos \theta_0 - \sqrt{2} v_2 |\lambda \mu_H^*| \cos \alpha_1 \cos \theta_2$$

$$+ \frac{v_1}{\sqrt{2}} \{ |\lambda \mu_\phi^*| \cos(\alpha_2 + \theta_1) + |m_3| \cos(\alpha_3 + \theta_1) \}, \quad (\text{B8})$$

$$\begin{aligned} \mathcal{M}_{24}^{0(0)} &= - \left(\frac{g^2 + g'^2}{2} - |\lambda|^2 \right) v_1 v_2 \sin \theta_1 \cos \theta_2 \\ &\quad - \frac{v_0}{\sqrt{2}} \{ |\lambda \mu_\phi^*| \sin(\alpha_2 - \theta_0) + |m_3| \sin(\alpha_3 + \theta_0) \}, \end{aligned} \quad (\text{B9})$$

$$\mathcal{M}_{25}^{0(0)} = \frac{g^2 + g'^2}{4} v_2^2 \sin 2\theta_2, \quad (\text{B10})$$

$$\begin{aligned} \mathcal{M}_{26}^{0(0)} &= |\lambda|^2 v_2 v_0 \cos \theta_2 \sin \theta_0 + \sqrt{2} v_2 |\lambda \mu_H^*| \sin \alpha_1 \cos \theta_2 \\ &\quad + \frac{v_1}{\sqrt{2}} \{ |\lambda \mu_\phi^*| \sin(\alpha_2 + \theta_1) - |m_3| \sin(\alpha_3 + \theta_1) \}, \end{aligned} \quad (\text{B11})$$

$$\mathcal{M}_{33}^{0(0)} = M_3^2 + \frac{|\lambda|^2}{2} (v_1^2 + v_2^2) - |m_2^2| \quad (\text{B12})$$

$$\begin{aligned} \mathcal{M}_{34}^{0(0)} &= |\lambda|^2 v_1 v_0 \sin \theta_1 \cos \theta_0 - \sqrt{2} v_1 |\lambda \mu_H^*| \cos \alpha_1 \sin \theta_1 \\ &\quad - \frac{v_2}{\sqrt{2}} \{ |\lambda \mu_\phi^*| \sin(\alpha_2 + \theta_2) + |m_3| \sin(\alpha_3 + \theta_2) \}, \end{aligned} \quad (\text{B13})$$

$$\begin{aligned} \mathcal{M}_{35}^{0(0)} &= |\lambda|^2 v_2 v_0 \sin \theta_2 \cos \theta_0 - \sqrt{2} v_2 |\lambda \mu_H^*| \cos \alpha_1 \sin \theta_2 \\ &\quad - \frac{v_1}{\sqrt{2}} \{ |\lambda \mu_\phi^*| \sin(\alpha_2 + \theta_1) + |m_3| \sin(\alpha_3 + \theta_1) \}, \end{aligned} \quad (\text{B14})$$

$$\mathcal{M}_{36}^{0(0)} = 0, \quad (\text{B15})$$

$$\begin{aligned} \mathcal{M}_{44}^{0(0)} &= M_1^2 + \frac{g^2 + g'^2}{4} v_1^2 (1 + 2 \sin^2 \theta_1) - \left(\frac{g^2 + g'^2}{4} - \frac{|\lambda|^2}{2} \right) v_2^2 \\ &\quad + \frac{|\lambda|^2}{2} v_0^2 - \sqrt{2} v_0 |\lambda \mu_H^*| \cos(\alpha_1 + \theta_0), \end{aligned} \quad (\text{B16})$$

$$\begin{aligned} \mathcal{M}_{45}^{0(0)} &= - \left(\frac{g^2 + g'^2}{2} - |\lambda|^2 \right) v_1 v_2 \sin \theta_1 \sin \theta_2 + |m_1^2| \\ &\quad - \frac{v_0}{\sqrt{2}} \{ |\lambda \mu_\phi^*| \cos(\alpha_2 - \theta_0) + |m_3| \cos(\alpha_3 + \theta_0) \}, \end{aligned} \quad (\text{B17})$$

$$\begin{aligned} \mathcal{M}_{46}^{0(0)} &= |\lambda|^2 v_1 v_0 \sin \theta_1 \sin \theta_0 + \sqrt{2} v_1 |\lambda \mu_H^*| \sin \alpha_1 \sin \theta_1 \\ &\quad + \frac{v_2}{\sqrt{2}} \{ |\lambda \mu_\phi^*| \cos(\alpha_2 + \theta_2) - |m_3| \cos(\alpha_3 + \theta_2) \}, \end{aligned} \quad (\text{B18})$$

$$\begin{aligned} \mathcal{M}_{55}^{0(0)} &= M_2^2 + \frac{g^2 + g'^2}{4} v_2^2 (1 + 2 \sin^2 \theta_2) - \left(\frac{g^2 + g'^2}{4} - \frac{|\lambda|^2}{2} \right) v_1^2 \\ &\quad + \frac{|\lambda|^2}{2} v_0^2 - \sqrt{2} v_0 |\lambda \mu_H^*| \cos(\alpha_1 + \theta_0), \end{aligned} \quad (\text{B19})$$

$$\begin{aligned} \mathcal{M}_{56}^{0(0)} &= |\lambda|^2 v_2 v_0 \sin \theta_2 \sin \theta_0 + \sqrt{2} v_2 |\lambda \mu_H^*| \sin \alpha_1 \sin \theta_2 \\ &\quad + \frac{v_1}{\sqrt{2}} \{ |\lambda \mu_\phi^*| \cos(\alpha_2 + \theta_1) - |m_3| \cos(\alpha_3 + \theta_1) \}, \end{aligned} \quad (\text{B20})$$

$$\mathcal{M}_{66}^{0(0)} = M_3^2 + \frac{|\lambda|^2}{2} (v_1^2 + v_2^2) + |m_2^2|, \quad (\text{B21})$$

$$\mathcal{M}_{22}^{0(1)} = \frac{3}{8\pi^2} \frac{m_t^4}{v_2^2} \cos^2 \theta_2 \log \frac{M_{t1}^2 M_{t2}^2}{m_t^4}, \quad (\text{B22})$$

$$\mathcal{M}_{55}^{0(1)} = \frac{3}{8\pi^2} \frac{m_t^4}{v_2^2} \sin^2 \theta_2 \log \frac{M_{t1}^2 M_{t2}^2}{m_t^4}, \quad (\text{B23})$$

$$\mathcal{M}_{25}^{0(1)} = \frac{3}{8\pi^2} \frac{m_t^4}{v_2^2} \sin \theta_2 \cos \theta_2 \log \frac{M_{t1}^2 M_{t2}^2}{m_t^4}, \quad (\text{B24})$$

where the extremum conditions in Eqs. (A1)-(A5) are not taken into account. The indices i, j ($=1-6$) are in order of $(h_R^1, h_R^2, \phi_R, h_I^1, h_I^2, \phi_I)$.

Appendix C: Mass-squared matrix for the charged Higgs bosons

The mass-squared matrix \mathcal{M}^\pm for the charged Higgs bosons receives contributions dominantly from the tree-level potential. The elements M_{ij}^\pm are given by

$$\begin{aligned} \mathcal{M}_{11}^\pm &= M_1^2 + \frac{g^2 + g'^2}{4} v_1^2 + \left(\frac{g^2 - g'^2}{4} + |\lambda|^2 \right) v_2^2 + \frac{|\lambda|^2}{2} v_0^2 \\ &\quad + \sqrt{2} |\lambda \mu_H^*| v_0 \cos(\alpha_1 + \theta_0), \end{aligned} \quad (\text{C1})$$

$$\begin{aligned} \mathcal{M}_{12}^\pm &= \frac{g^2 + |\lambda|^2}{2} v_1 v_2 \exp[i(\theta_1 + \theta_2)] + |m_1^2| \\ &\quad + \frac{v_0}{\sqrt{2}} \{ |\lambda \mu_\phi^*| \exp[-i(\alpha_2 - \theta_0)] + |m_3| \exp[-i(\alpha_3 + \theta_0)] \}, \end{aligned} \quad (\text{C2})$$

$$\begin{aligned} \mathcal{M}_{13}^\pm &= \frac{g^2 - |\lambda|^2}{\sqrt{2}} v_1 v_0 \exp[i(\theta_1 - \theta_0)] - v_1 |\lambda \mu_H^*| \exp[i(\alpha_1 + \theta_1)] \\ &\quad + v_2 |\lambda \mu_\phi^*| \exp[-i(\alpha_2 + \theta_2)], \end{aligned} \quad (\text{C3})$$

$$\begin{aligned} \mathcal{M}_{14}^\pm &= -\frac{g^2 - |\lambda|^2}{\sqrt{2}} v_1 v_0 \exp[i(\theta_1 + \theta_0)] - v_1 |\lambda \mu_H^*| \exp[-i(\alpha_1 - \theta_1)] \\ &\quad + v_2 |m_3| \exp[-i(\alpha_3 + \theta_2)], \end{aligned} \quad (\text{C4})$$

$$\begin{aligned} \mathcal{M}_{22}^\pm &= M_2^2 + \left(\frac{g^2 - g'^2}{4} + |\lambda|^2 \right) v_1^2 + \frac{g^2 + g'^2}{4} v_2^2 + \frac{|\lambda|^2}{2} v_0^2 \\ &\quad + \sqrt{2} v_0 |\lambda \mu_H^*| \cos(\alpha_1 + \theta_0), \end{aligned} \quad (\text{C5})$$

$$\begin{aligned} \mathcal{M}_{23}^\pm &= \frac{g^2 - |\lambda|^2}{\sqrt{2}} v_2 v_0 \exp[-i(\theta_2 + \theta_0)] + v_2 |\lambda \mu_H^*| \exp[i(\alpha_1 - \theta_2)] \\ &\quad - v_1 |m_3| \exp[i(\alpha_3 + \theta_1)], \end{aligned} \quad (\text{C6})$$

$$\begin{aligned} \mathcal{M}_{24}^\pm &= -\frac{g^2 - |\lambda|^2}{\sqrt{2}} v_2 v_0 \exp[-i(\theta_2 - \theta_0)] + v_2 |\lambda \mu_H^*| \exp[-i(\alpha_1 + \theta_2)] \\ &\quad - v_1 |\lambda \mu_\phi^*| \exp[i(\alpha_2 + \theta_1)], \end{aligned} \quad (\text{C7})$$

$$\mathcal{M}_{33}^\pm = M_3^2 - \left(\frac{g^2}{2} - |\lambda|^2 \right) v_1^2 + \frac{g^2}{2} v_2^2 + g^2 v_0^2, \quad (\text{C8})$$

$$\mathcal{M}_{34}^\pm = -g^2 v_0^2 \exp[2i\theta_0] - |m_2^2|, \quad (\text{C9})$$

$$\mathcal{M}_{44}^\pm = M_3^2 + \frac{g^2}{2} v_1^2 - \left(\frac{g^2}{2} - |\lambda|^2 \right) v_2^2 + g^2 v_0^2, \quad (\text{C10})$$

where the extremum conditions in Eqs. (A1)-(A5) are not taken into account. The indices i, j ($=1-4$) are in order of $(h_1^-, h_2^{+*}, \phi^-, \phi^{+*})$.

-
- [1] ATLAS Collaboration, Phys. Lett. **B 716**, 1 (2012);
CMS Collaboration, Phys. Lett. **B 716**, 30 (2012).
 - [2] CDF and D0 Collaborations, Phys. Rev. **D 88**, 052014 (2013);
ATLAS and CMS Collaborations, Phys. Rev. Lett. **114**, 191803 (2015);
ATLAS Collaboration, JHEP **08**, 045 (2016);
CMS Collaboration, JHEP **11**, 047 (2017);
ATLAS Collaboration, Phys. Rev. Lett. **119**, 051802 (2017);
ATLAS Collaboration, JHEP **12**, 024 (2017).
 - [3] ACME Collaboration, Science **343**, 269 (2014).
 - [4] J. M. Pendlebury *et al.* Phys. Rev. **D 92**, 092003 (2015).
 - [5] S.M. Barr and A. Zee, Phys. Rev. Lett. **65**, 21 (1990).
 - [6] A. Pilaftsis, Phys. Lett. **B 435**, 88 (1998);
M. Carena, J. Ellis, A. Pilaftsis, and C.E.M. Wagner, Phys. Lett. **B 495**, 155 (2000).
 - [7] N. Oshimo, Phys. Rev. **D 93**, 095017 (2016).
 - [8] Y. Okada, M. Yamaguchi, and T. Yanagida, Prog. Theor. Phys. **85**, 1 (1991);
J. Ellis, G. Ridolfi, and F. Zwirner, Phys. Lett. **B 257**, 83 (1991);
H.E. Haber and R. Hempfling, Phys. Rev. Lett. **66**, 1815 (1991).
 - [9] Particle Data Group, Phys. Rev. **D 98**, 030001 (2018).
 - [10] See, *e.g.*, B.A. Kniehl, Phys. Rep. **240**, 211 (1994).
 - [11] CMS collaboraion, JHEP **10**, 144 (2015).
 - [12] ALEPH, DELPHI, L3, and OPAL Collaborations, Eur. Phys. J. **C 73**, 2463 (2013).